Thermo-mechanical and Atomistic Assessment of First Wall, and Optics in non-protective chamber in Inertial Fusion Energy

J M Perlado, A Rivera, R González-Arrabal, O. Peña, D Garoz*, M. Panizo

Instituto de Fusión Nuclear, ETSII, Universidad Politécnica de Madrid, Spain.

** also, Mechanics of Material and Structures, Ghent University*

josemanuel.perlado@upm.es

SUMMARY

THERMOMECHANICAL EFFECTS FOR DIFFERENT IFE REACTOR ASSUMPTIONS: DEFINING FW THICKNESS

GRAIN BOUNDARIES EFFECTS IN H BEHAVIOUR: COMPUTATION AND EXPERIMENTS

EFFECTS OF PLASMONIC NANOPARTICLES IN OPTICS BEHAVIOUR

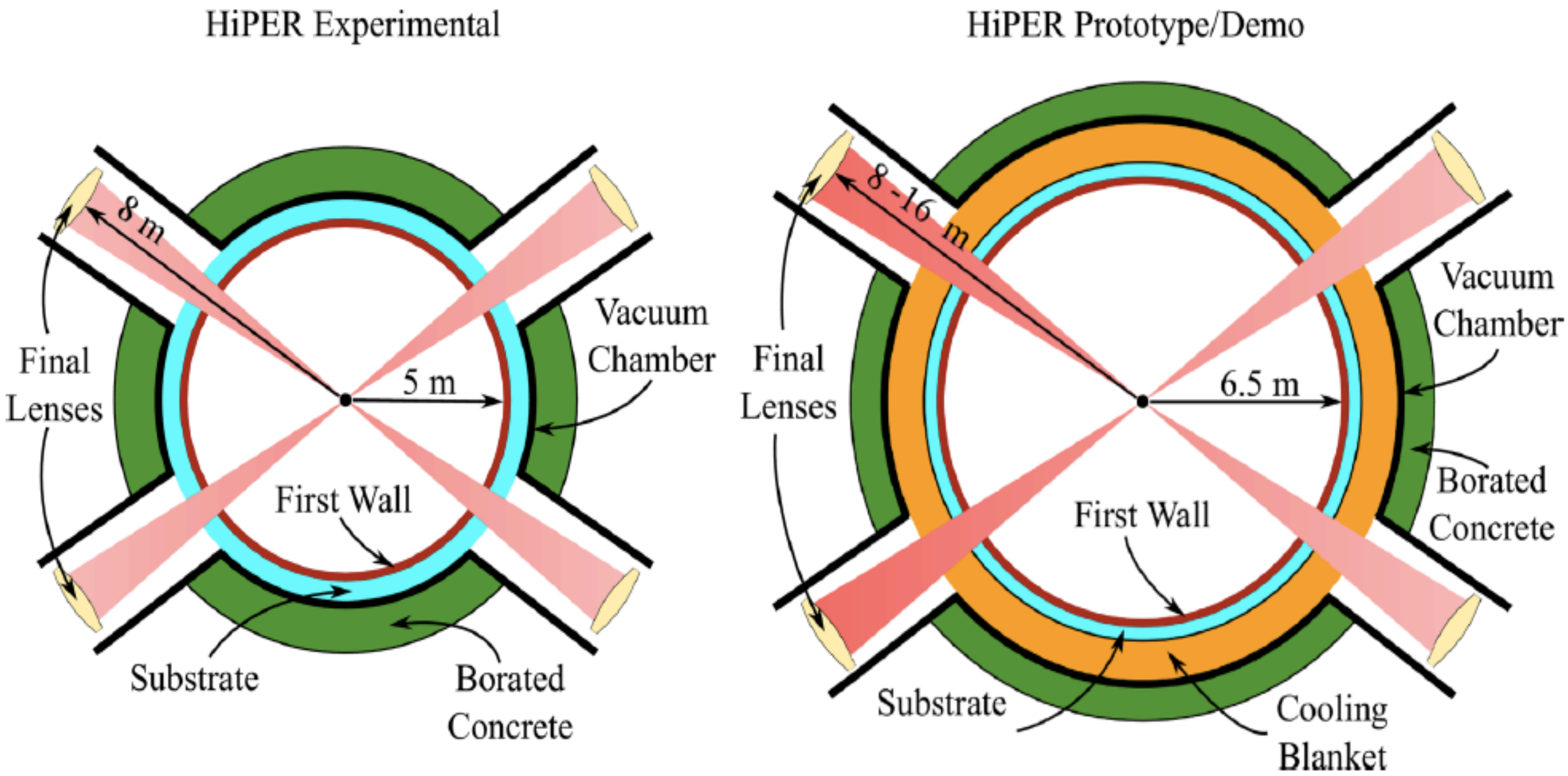
HiPER Experimental
8 m
Final
Lenses
5 m
Vacuum
Chamber
First Wall
Substrate
Borated
Concrete
HiPER Prototype/Demo
8 -16 m
Final
Lenses
6.5 m
Vacuum
Chamber
Borated
Concrete
First Wall
Substrate
Cooling
Blanket

Working parameters for HiPER different schemes of implementation

Parameter	Experimental	Prototype	Demo
Frequency	Few shots per bunch	1 Hz	10 Hz
Shot energy (MJ)	20	50	154
Chamber radius (m)	5	6.5	6.5

more details in Garoz et al, Nuclear Fusion

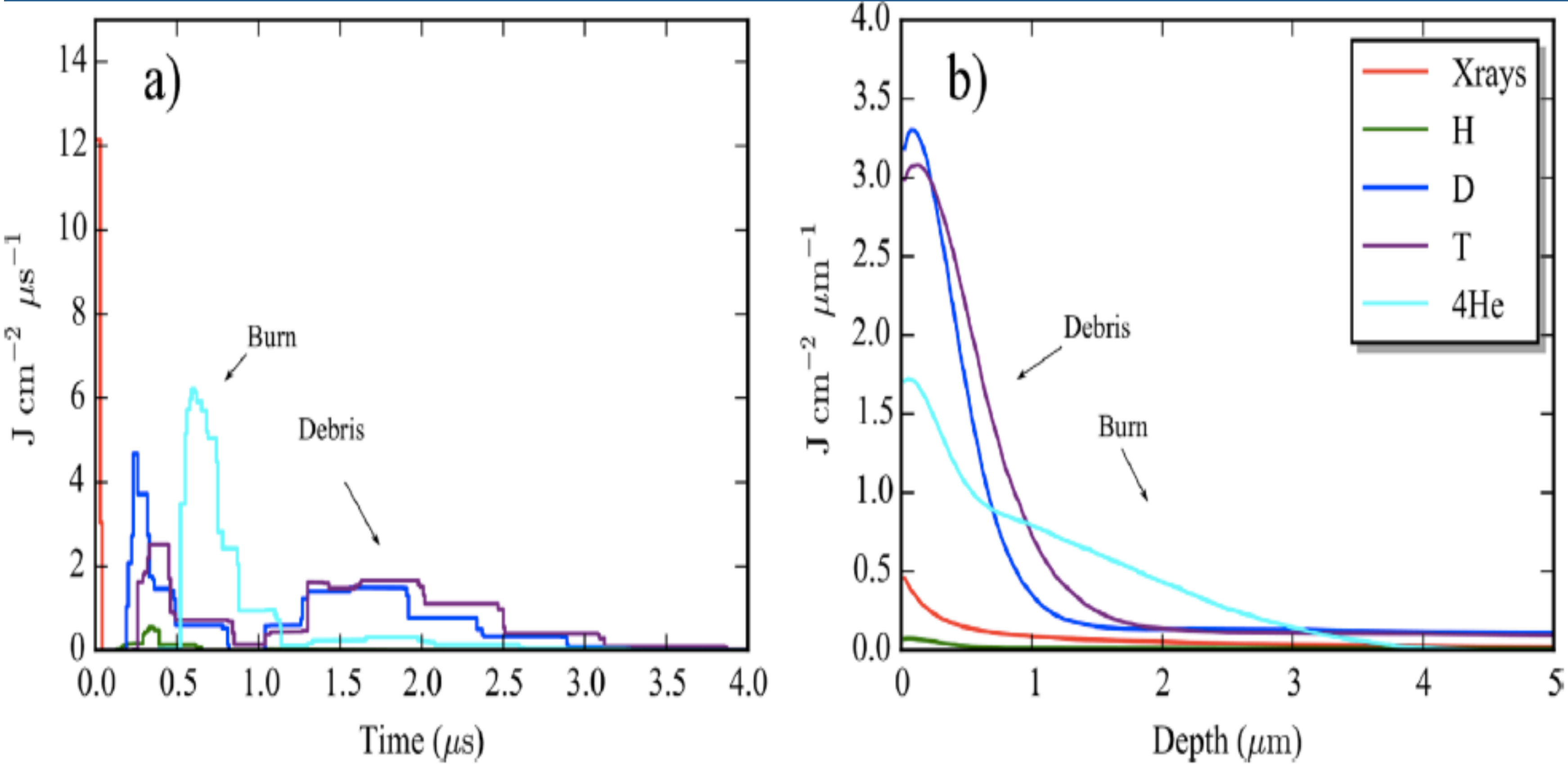

10 % of Energy is deposited within depths up to 100 µm by the most energetic ions (> 1 MeV).

Deposition of Energy in FW from Target in Direct Drive DEMO HiPER

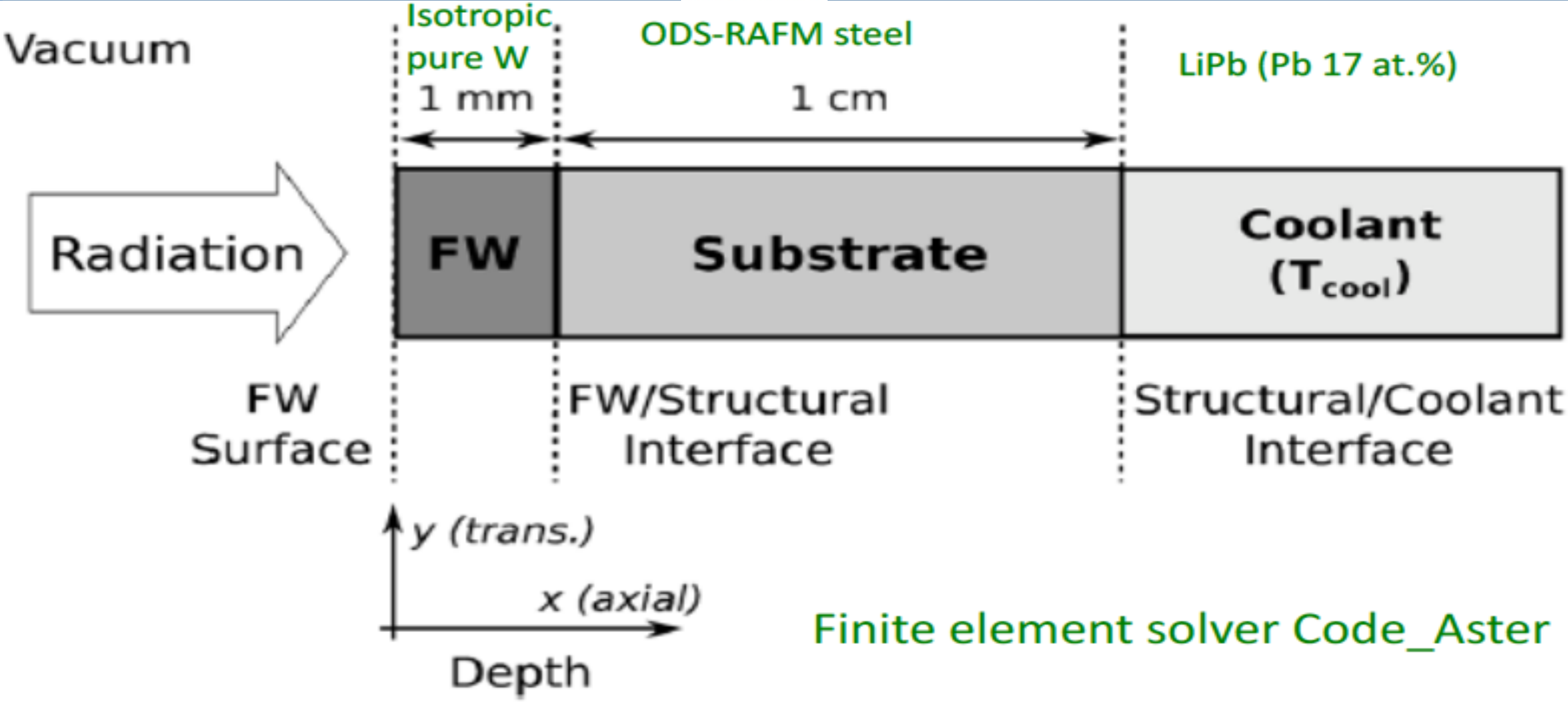

Finite element solver Code_Aster

For fracture analysis:
the stress intensity factors (K) are calculated
using the singular displacements method implemented in the
CALC_G module of Code_Aster

Several aspects need to be considered when estimating the required W thickness for the FW:

- The stopping of ions in order to keep them away from the substrate (≥ 100 μm)

- From the thermomechanical point of view, the accommodation of the stresses generated in the FW, which requires a thickness of ~100 μm in order to accommodate the plastic Stresses, and

- ***Crack propagation along the FW, to prevent undesired growth up to the substrate.***

Reactor "start-up" times:

lower than ~6 s for Prototype (1 Hz, 50 MJ)

and

~60 s for Demo (10 Hz, 154 MJ)

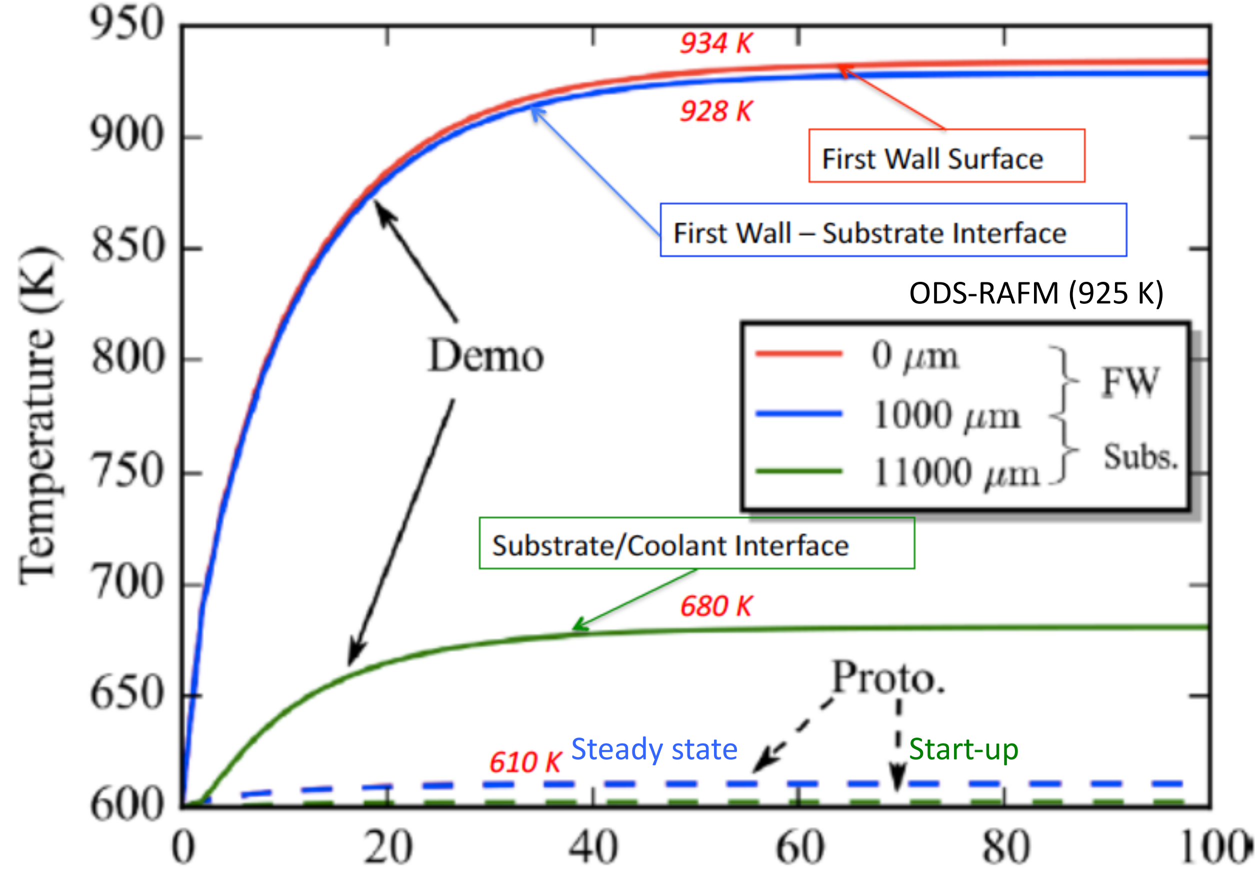

Time during the start-up for the HiPER Proto and Demo

Two situations:

"start up"

and

Steady state

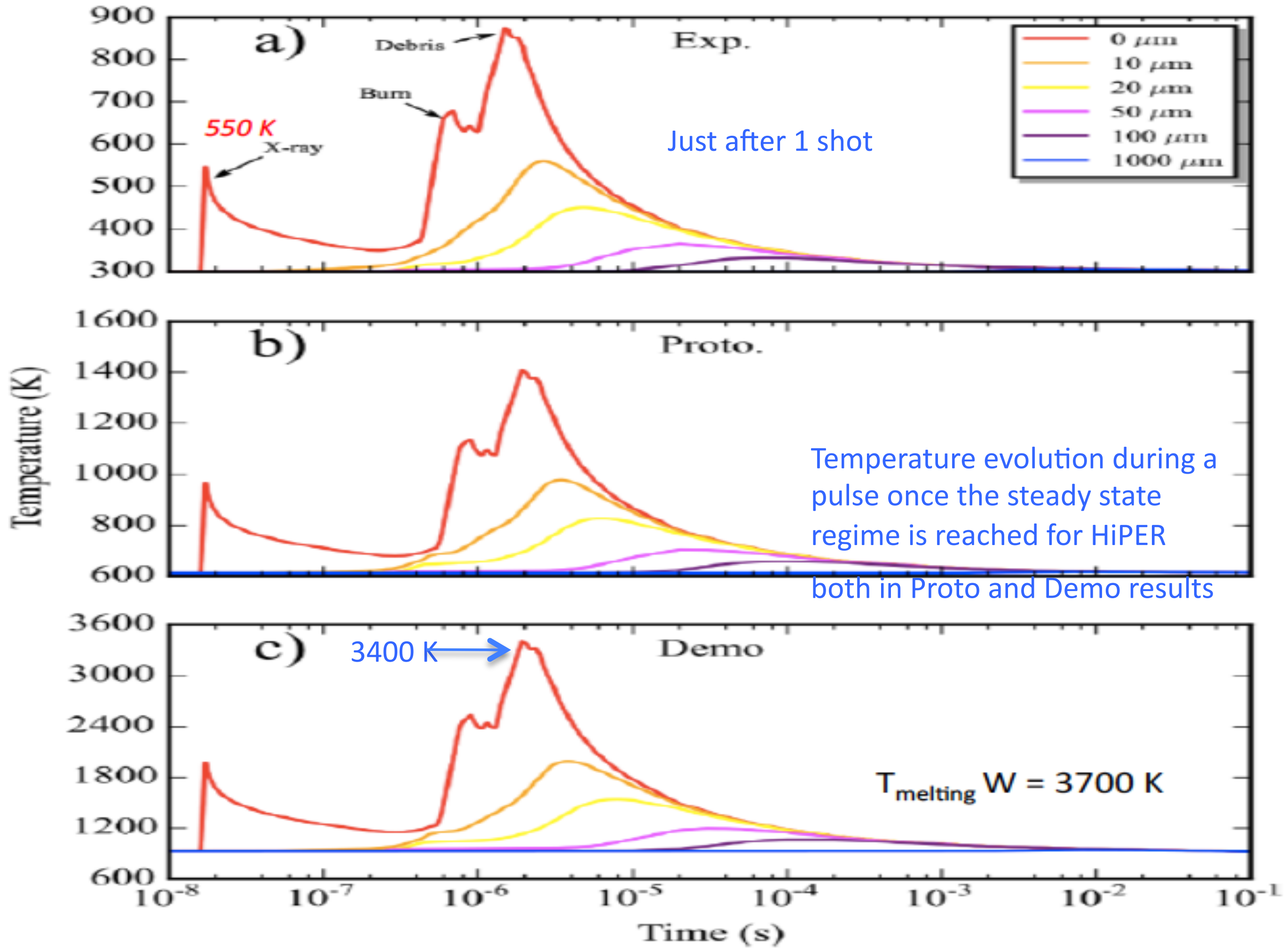

Temperature evolution during a pulse once the steady state regime is reached for HiPER both in Proto and Demo results

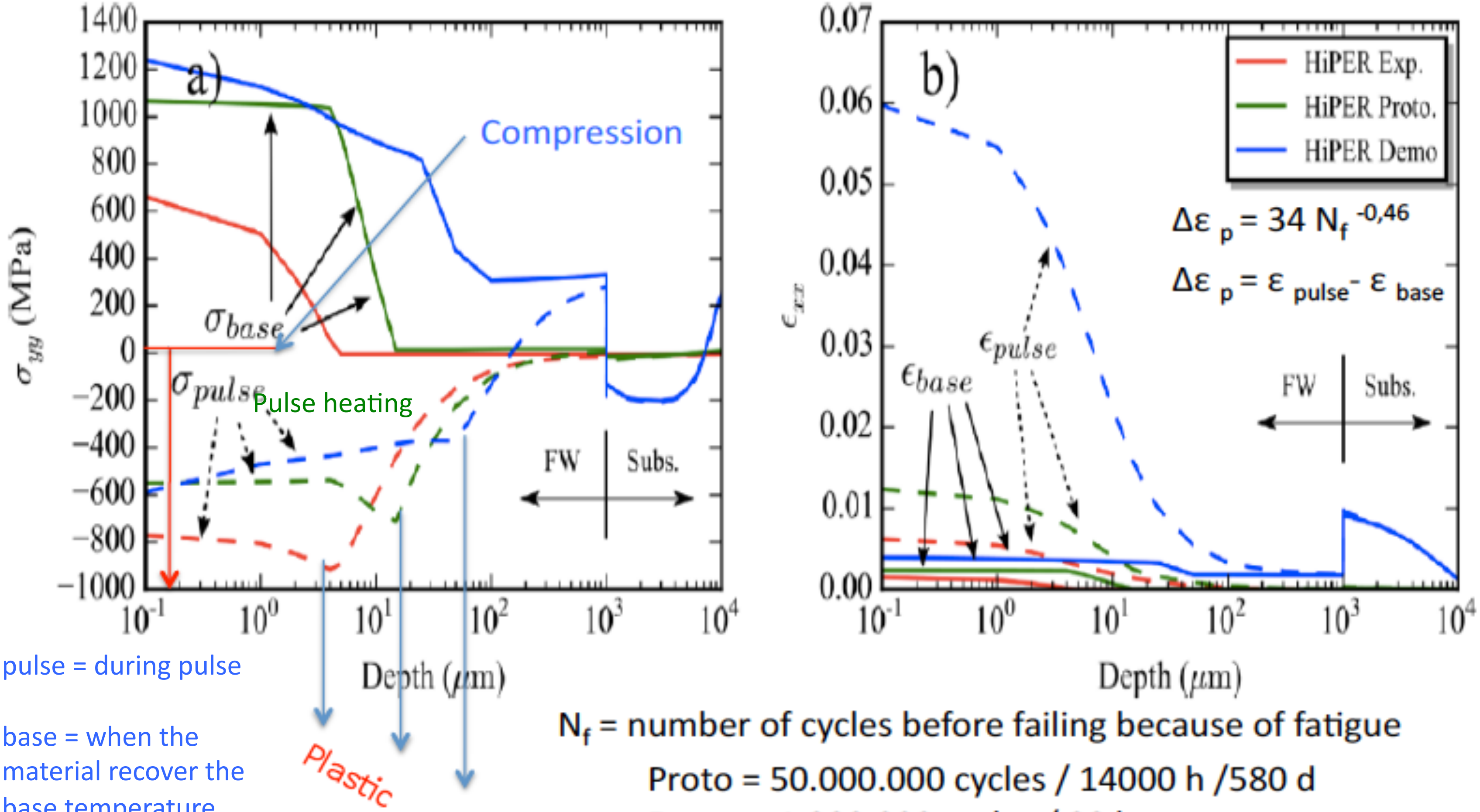

pulse = during pulse

base = when the material recover the base temperature

N_f = number of cycles before failing because of fatigue

Proto = 50.000.000 cycles / 14000 h /580 d

Demo = 1.000.000 cycles / 28 h

Transverse Stress

Axial Strain

Effects of Thermo-mechanical effects of FW Irradiation have been established

Based on realistic studies of Target emissions transport and deposition in the FW.

A well defined thickness of FW is designed under the knowledge of potential limiting processes.

- How GBs affect radiation-induced defect configuration?
  - RT, T>RT

- How GBs affect light species behavior?
  - RT, T>RT

- Influence of the geometry of the grain boundaries?
- Accommodation limit? → Mechanical properties?
- Operational windows for the self-healing mechanism?
- Operational temperature range for nanostructured tungsten?

Sample code	Structure
NW-H	Nano
CGW-H	Coarse grained
NW-Se-CH	Nano
CGW-Se-CH	Coarse grained
NW-Co-CH	Nano
CGW-Co-CH	Coarse grained

- Implantations were selected to mimic as much as possible IFE conditions J. Alvarez *et al.* Fusion Engineering and Design 86 (2011) 1762–1765
  - Sequential implantation: **C** (665KeV@RT) **plus H** (170KeV@RT)

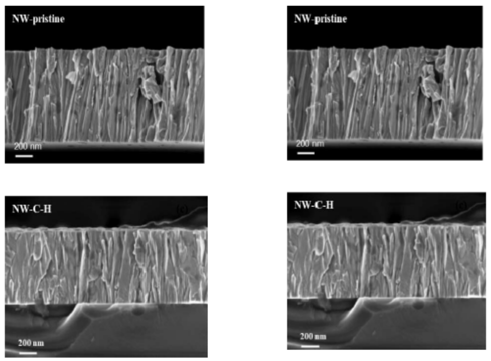

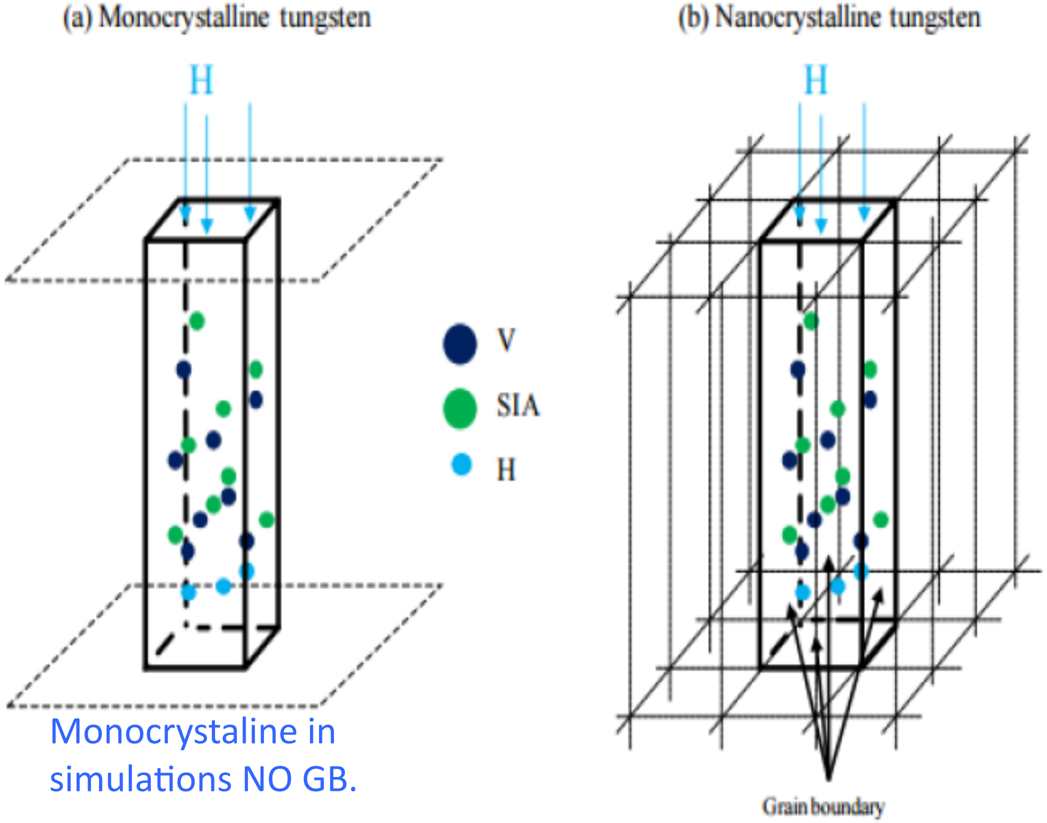

Monocrystaline in simulations NO GB.

G. Valles et al. Acta Mater. 122 (2017) 277–286
C. Gonzalez *et al.* Nuclear Fusion 55(11):113009, 2015

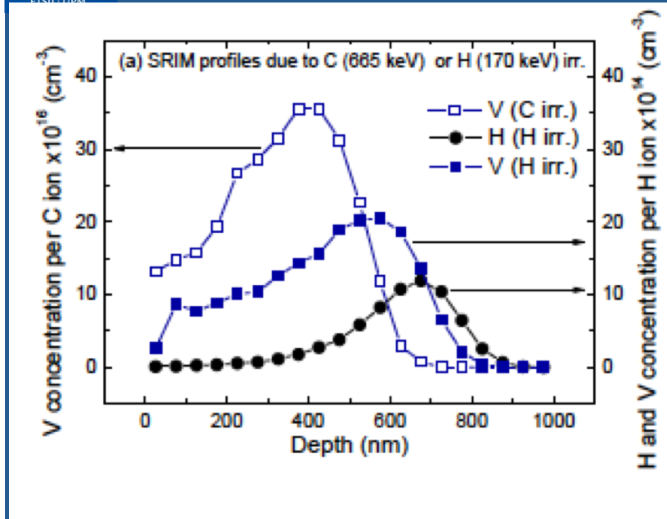

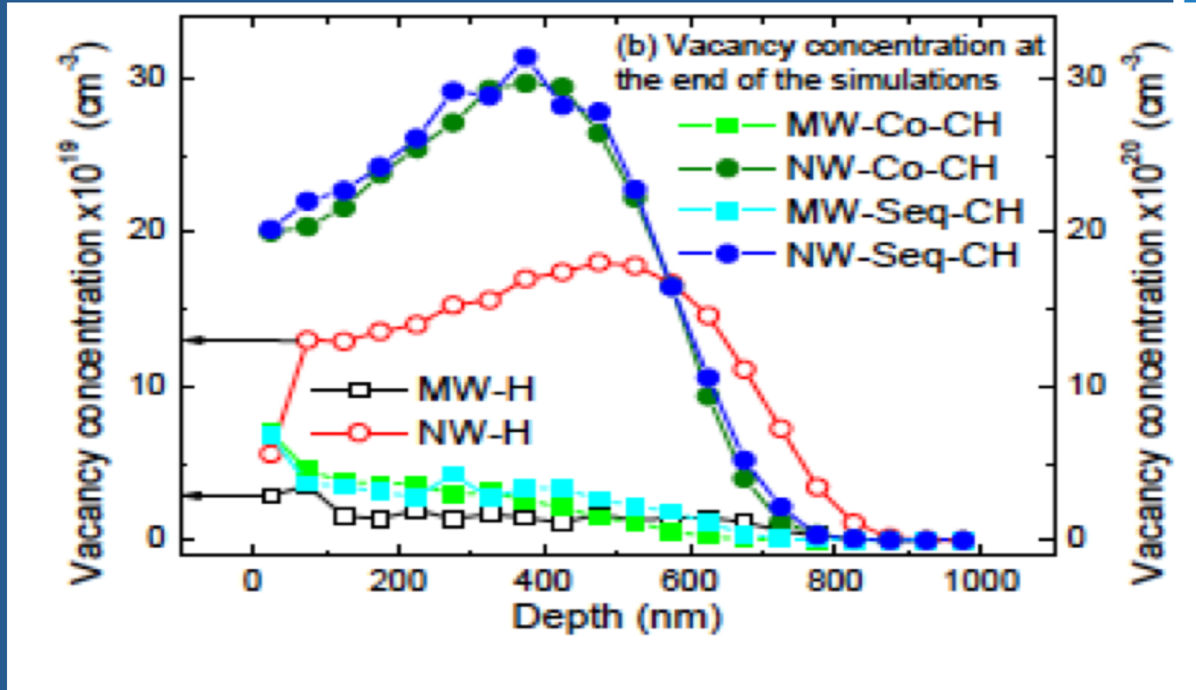

GBs dramatically affect the vacancy concentration, being much higher for samples with a large GB density than for those without GBs. The key reason is that most of the vacancies annihilate with SIAs in absence of GBs, whereas in NW, at this temperature in which vacancies are immobile, a larger fraction of vacancies survives after the irradiation due to the efficient role of GBs as sinks for SIAs.

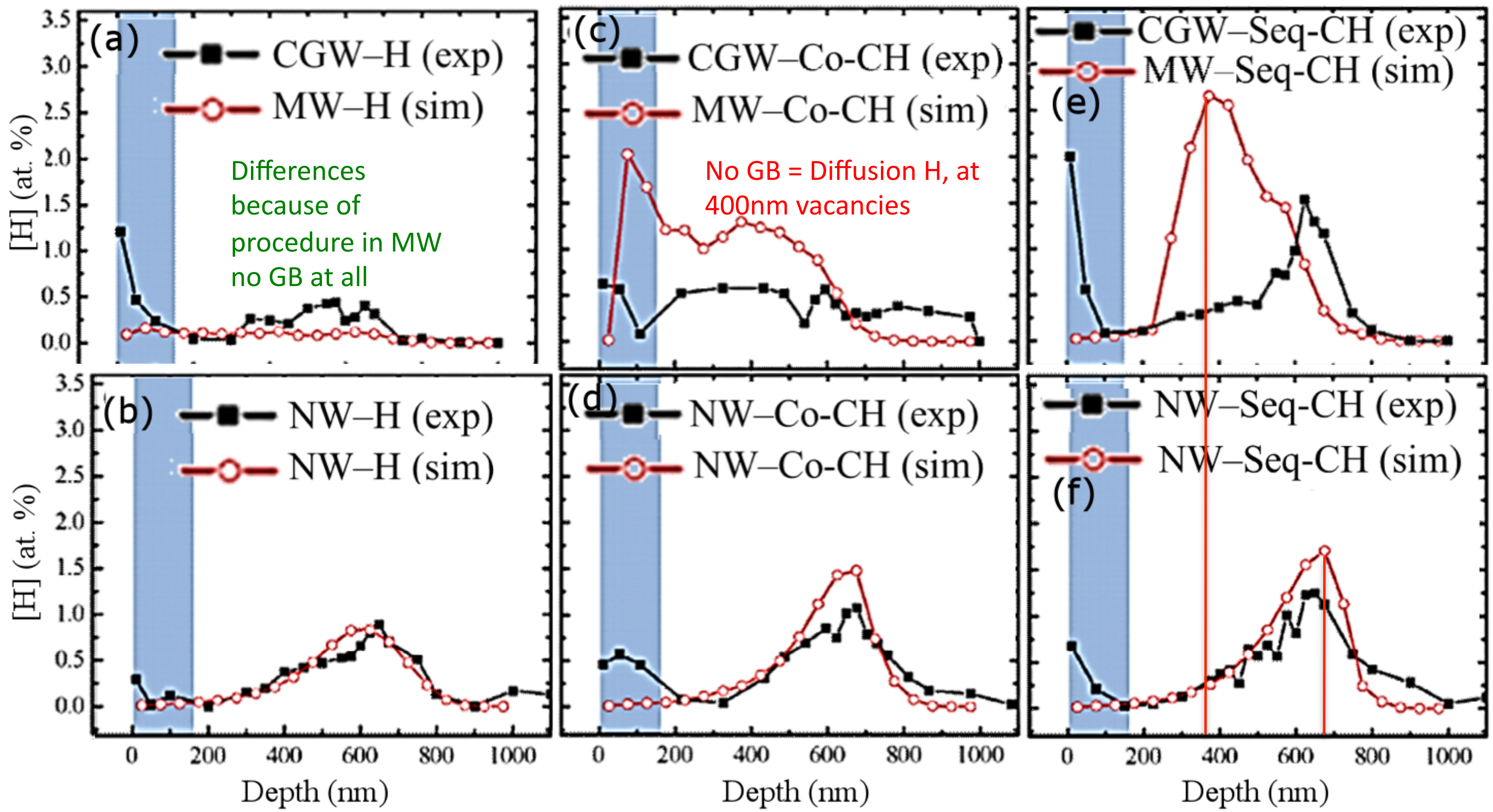
(a)
CGW–H (exp)
MW–H (sim)
Differences because of procedure in MW no GB at all
(c)
CGW–Co-CH (exp)
MW–Co-CH (sim)
No GB = Diffusion H, at 400nm vacancies
CGW–Seq-CH (exp)
MW–Seq-CH (sim)
(e)
(b)
NW–H (exp)
NW–H (sim)
(d)
NW–Co-CH (exp)
NW–Co-CH (sim)
NW–Seq-CH (exp)
NW–Seq-CH (sim)
(f)
[H] (at. %)
Depth (nm)

(a) Differences are observed when comparing results for the CGW to those for the MW samples. The reason is that the simulations (MW) do not consider GBs at all, whereas some GBs exist in the CGW sample.

(b) For NW-H, results clearly indicates H diffusion along the depth direction.

(c) For the MW-Co-CH, the main H retention peak locates at ~400 nm. This result indicates that in the absence of GBs, H atoms diffuse along the irradiation direction, and in their migration to the surface, H atoms reach a region highly populated by vacancies at ~400 nm, where they get trapped, explaining the differences in the H profile between 150 and 540 nm.

(d) For NW-Co-CH, there is good agreement between measured and simulated H profile. In addition, the total H retention is almost the same in the simulations as in the experiments and diffusion is observed.

(f) The measured and simulated H profiles agree quite well for the NW-Seq-CH. Both profiles show H retention peak at ~650 nm. Moreover, the total measured and simulated retained fractions are quite similar.

When Sequential C-H, we observe that the enhancement for the NW is lower than that for the MW samples. This supports the idea of the GBs acting as diffusion paths for H. The presence of a higher GB density in NW leads to a higher probability of H release along GBs, being less affected by the presence of the higher vacancy concentrations induced by C irradiation.

When comparing the data for the MW-Co-CH and for the MW-Seq-CH, we observe a clear influence of the irradiation procedure itself on the H retention, even though the concentration of vacancies is similar in both cases.

H atoms are mainly trapped in vacancies located in the interior of the grains. The next question is to estimate the type and size of clusters where H atoms are trapped. Study is on going experimentally *(M. Panizo et al., to be published)*

According to our simulations, since vacancies are immobile at RT, more than 90% of H atoms are retained in monovacancies with different H content. Moreover, DFT data show that that the maximum number of H atoms that can be accommodated inside the monovacancy is 10. From these data we can conclude that self-healing in W would happen at temperatures in which the mobility of vacancies is activated.

This remark, together with the fact that GBs favors H release, indicate that nanostructured W may be a candidate for PFM applications, as it has a higher radiation resistance than the traditionally CGW

Plasmonic Nanoparticles *and* Optics

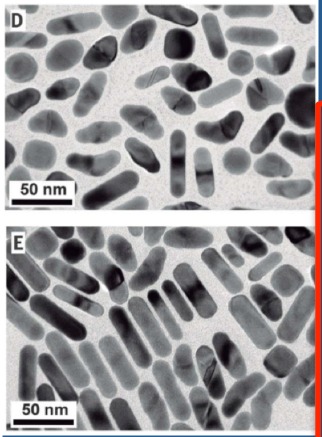

G. Gonzalez-Rubio**, O. Peña-Rodriguez et al.,** Femtosecond laser reshaping yields gold nanorods with ultranarrow surface plasmon resonantes, Science 358, 640, 2017

O. Peña-Rodríguez, et al., Understanding the ion-induced elongation of silver nanoparticles embedded in silica, Nature Scientific Reports, 7: 922, 2017

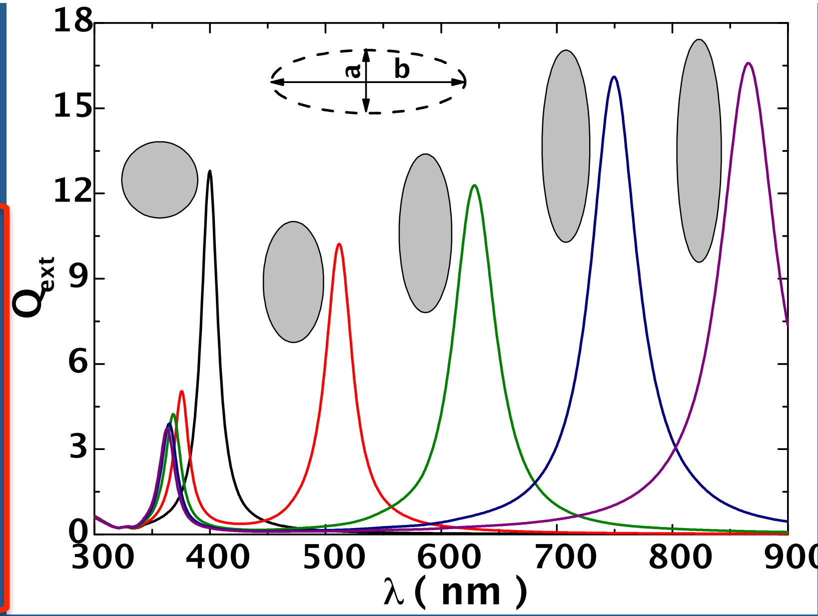

The irradiation of gold nanorod colloids with a femtosecond laser can be tuned to induce controlled nanorod reshaping, yielding colloids with exceptionally narrow localized surface plasmon resonance bands.

Highly concentrated silver colloidal nanoparticle solutions were produced thanks to fs laser ablation and it was demonstrated that such embedded plasmonic nanoparticles may be viable candidates to reduce damages produced on optics by swift heavy ions due to the change of their shape under irradiation

INDUSTRIALES ETSII | UPM

IFN Instituto de Fusión Nuclear

POLITÉCNICA "Ingeniamos el futuro"

D. Garoz, A.R. Páramo, A. Rivera, J.M. Perlado and R. González-Arrabal, Nucl. Fusion 56 (2016) 126014 (11pp)

R. Gonzalez-Arrabal *et al.* JNM 453(1–3):287–295

P. Piaggi *et al.* JNM 458:233–239, 2015.

C. Gonzalez *et al.* Nuclear Fusion 55(11):113009, 2015

G. Valles *et al.* NIMB 352:100–103, 2015

C. Guerrero *et al.* Journal of Materials Science 51(3):1445–1455, 2015

G. Valles *et al.* JNM 457:80–87, 2015

G. Valles *et al.* Acta Materialia 122 (2017) 277-286

ACKNOWLEDGEMENT

Work under National Research RADIAFUS ENE-2012-39787-CO6,

Madrid Government TECHNOFUSION (II)-CM, S2013/MAE-2745, and

Eurofusion ToIFE Project AWP15-ENR-01/CEA-02